Full-field photonic biosensors based on tunable bio-doped sol–gel glasses

Andreu Llobera,[a] Victor J. Cadarso,[a] Margarita Darder,[b] Carlos Domínguez[a] and César Fernández-Sánchez*[a]

Received 22nd January 2008, Accepted 23rd April 2008
First published as an Advance Article on the web 23rd May 2008
DOI: 10.1039/b801152d

A full-field generic photonic biosensor approach, which relies on a bio-doped polymeric strip waveguide configuration, is described. We show the potential of tailor-made hybrid polymeric materials prepared by sol–gel technology for the fabrication of ultra-compact biosensor devices, where both the transducer and the recognition elements are merged into one single microstructure. Such devices were fabricated by micromolding in capillaries (MIMIC) soft lithographic technique. In contrast to evanescent field sensors, the sensor response does not only rely on the interaction of the evanescent wave with the recognition element, but on the interaction of the whole field, thus enabling a reduction of the sensor dimensions and/or a decrease of its limit of detection (LOD). The potential of this generic approach was demonstrated by developing a biosensor for the detection of H_2O_2 using horseradish peroxidase (HRP) as the doping agent. Solutions containing 2,2′-azino-bis(3-ethylbenzothiazoline-6-sulfonic) acid (ABTS) and different concentrations of H_2O_2 were dispensed over the waveguide and the green-coloured cation radical $ABTS^{\bullet+}$ product was mainly obtained inside the photonic structure, resulting in a maximum absorption increase of 2.5 a.u. at a set working wavelength of 670 nm over the H_2O_2 concentration range studied. The sensor exhibited a sensitivity of $(3.1 \pm 0.2) \times 10^3$ a.u./mol L^{-1} and a limit of detection (LOD) of 4.4×10^{-5} mol L^{-1} H_2O_2. These results anticipate that full-field waveguide microstructures based on bio-doped sol–gel polymers will enable the fabrication of cost-effective photonic biosensors. Moreover, the ease of fabrication by a soft lithography technique and the use of such polymeric materials are fully compatible with their integration in compact automatic analysis systems.

1. Introduction

Over the past few years a variety of smart materials have been applied for the definition of photonic lab-on-a-chip systems. These include tailor-made polymeric structures exhibiting very interesting properties, such as high transparency, strict control over the refractive index, easy deposition as thick layers, low processing temperature, compatibility with the integrated circuits technology, and low cost. The latter is one of the main drawbacks that make quite well established technologies for the fabrication of such systems not to be beyond pure research work. One example is the development of lab-on-a-chip approaches using silicon nitride structures.[1] Herein, the nanometre-scale technological requirements for implementing such photonic systems make it extremely difficult to hold the low cost assumption. The use of polymeric materials,[2] particularly organic–inorganic silicate-based glasses fabricated by sol–gel technology, which fulfil all the above-cited requirements,[3] is anticipated to overcome this drawback. In this context, a lot of effort has been made by different research groups to demonstrate the validity of these materials for photonic applications, from waveguides[4] to resonators.[5] Silica-based sol–gel materials also provide the rigid and compact matrix into which a large amount of different functional components, even from biological origin, can be easily incorporated. Thus, it is possible to obtain hybrid nanocomposites with additional functionalities, which may expand their application in fields where integration, miniaturization and multiparametric detection are added values.

Lately, the field of nanophotonics has devoted much interest among the scientific community. Here, sol–gel matrixes doped with either inorganic or organic materials have also been reported for the development of photonic devices and systems. The former includes zirconia, to obtain waveguides,[6] multimode interference couplers[7] and distributed feedback lasers (DFB),[8] or erbium/ytterbium/aluminium for the fabrication of amplifiers.[9] An example of the latter is the application of azo-type chromophores, which enhance the electro-optic (EO) coefficient,[10] and rhodamine, also for the design of amplifiers.[5] Other organic dopants have also been proposed as receptors in the design of sol–gel based chemical sensors. Such receptors are sterically accessible to molecules and ions small enough to diffuse into the sol–gel porous structure. Yang and Saavedra[11] proposed a system that consisted of a sol–gel layer containing an indicator, coated over a planar integrated optical waveguide (IOW). By means of the evanescent field (EF), species selectively adsorbed by the indicator can be optically monitored. Such a system was optimized for both refractive index and fluorescence

[a]*Instituto de Microelectrónica de Barcelona, CNM-IMB (CSIC), Campus Universitat Autónoma de Barcelona, 08193, Bellaterra, Spain. E-mail: cesar.fernandez@cnm.es; Fax: +34 93 580 14 96; Tel: +34 93 594 77 00*
[b]*Instituto de Ciencia de Materiales de Madrid (ICMM-CSIC), 28049, Cantoblanco, Madrid, Spain*

detection.[12] Nevertheless, in planar waveguides light is only confined in the direction orthogonal to the surface, diverging in the parallel axes. Hence, such structures have to be as small as possible to ensure a high signal-to-noise ratio (SNR). Besides, they cannot be integrated into a densely-packed photonic system. In an attempt to overcome this limitation, various techniques for patterning sol–gel glasses have been proposed. These include UV-lithography,[13] reactive ion etching[14] and soft lithography.[4] Among the different soft lithographic approaches, micromolding in capillaries (MIMIC)[15] features several outstanding properties, such as high fidelity in transferring the patterns from the mould to the substrate or the flexibility of generating arbitrarily-shaped structures in the same chip. In this context, MIMIC has recently been applied to integrated optics and microoptics. Concretely, it has been used to define complex optical elements, such as diffraction gratings on the surface of spherical lenses.[15]

Despite the good performance of rib or strip sol–gel waveguides, up to date there has been no contribution concerning the development of photonic lab-on-a-chip systems using this material. This may be due to the loss of dimensions and/or the cracking of the structures during the ageing and drying processes. In this paper, we overcome the previously mentioned limitations and fabricated a biosensor based on bio-doped hybrid sol–gel materials in strip waveguide configuration. Indeed, using horseradish peroxidase (HRP) as the doping agent, an absorbance biosensor for the detection of hydrogen peroxide is described. Merging both transducer (waveguide) and recognition element (HRP) into one single microstructure would allow for the development of compact lab-on-a-chip systems in a one-step fabrication process. This is the first time, to the best of our knowledge, that such configuration is presented.

2. Experimental

2.1. Materials

Tetramethoxysilane (≥99.0%, TMOS), methyltrimethoxysilane (≥98.0%, MTMOS), phenyltrimethoxysilane (purum, PhTMOS) were purchased from Sigma–Aldrich, Química S.A. (Spain), and used as received. SU-8 2025 photocurable polymer and propylene glycol methyl ether acetate (PGMEA) developer were from Microresist Technology GmbH (Berlin, Germany). Sylgard Silicone Elastomer 184 and Sylgard Curing Agent 184 were from Dow Corning Corp (Midland, MI, USA). All other chemicals were of analytical reagent grade. Ultrapure water (resistivity, 18 MΩ cm) was also used.

2.2. Preparation of masters and molds

Masters were fabricated with the negative photoresist SU-8 by one photolithographic process. SU-8 2025 was used to obtain layers with thicknesses up to 25 μm by spin-coating at 3000 rpm for 30 s on a 4 inch SiO_2-coated Si wafer. Following a bake step at 95 °C for 1 h, the SU-8 layer was exposed to UV light through a mask for 12 s. A post-exposure bake at 95 °C for 15 min was then carried out, before developing the SU-8 in PGMEA to obtain the master.

PDMS prepolymer solution was made by thoroughly mixing 5 mL of the silicon elastomer 184 and 0.5 mL of the curing agent 184 (10 : 1 (v : v) ratio), respectively. The mixture was put under vacuum to remove air bubbles. Then, it was carefully poured onto the SU-8 master to cover its entire area, and finally cured at 80 °C for 30 min. Using these experimental conditions, the thickness of the PDMS was always less than 2 mm. The fabricated PDMS mould was peeled off the master with the aid of tweezers and stored in a closed container. The resulting PDMS was the size of the master (4 inches). Before use, the PDMS was cut in pieces (areas around 1 cm^2) containing the desired waveguides having both ends open, using a scalpel. All these processes were carried out under clean room conditions.

2.3. Sol–gel preparation

The sol solution was prepared by mixing 615 μL of MTMOS, 60 μL of TMOS and 75 μL of PhTMOS stock solutions, under constant stirring. Then, 2750 μL of water were added. These volumes gave a 10 : 1 : 1, MTMOS : TMOS : PhTMOS and a 1 : 30, silanes : water molar ratios. The resulting mixture was gently stirred for several hours, at room temperature, until it lost around 40% of its initial weight. Then, 100 μL of this solution was thoroughly mixed with 30 μL of a 1 mg mL^{-1} HRP solution in 0.05 M Tris–HCl buffer pH 7. The pH of the resulting solution was around 4.5. At this point, the resulting sol solution was homogeneous and ready for the patterning process.

2.4. Fabrication of waveguides by MIMIC process

Waveguides were fabricated on thermally-grown SiO_2/Si substrates. They were previously cleaned by immersion in concentrated sulfuric acid and then thoroughly rinsed with ultrapure water and ethanol, and dried under a stream of N_2. The PDMS mould (area around 1 cm^2), containing 20 μm-high waveguide structures having their ends open, was then stuck to the substrate. After that, 4 μL of the sol solution containing HRP was pipetted at one end of the structures and left to fill the waveguide channels by capillary action. This process took less than a minute. When the sol solution reached the other end of the waveguides, more sol solution was added on both ends, to prevent the structures from emptying. Then, the PDMS/substrate system was left undisturbed in a sealed container at 4 °C for at least three days to allow the polymer to gel and age. After that, the PDMS mould was peeled off the substrate with the aid of tweezers in order to release the doped sol–gel waveguide microstructures. Finally, in order to have good facet quality, the substrate was manually cleaved, removing the filling regions of the MIMIC process and hence achieving optical access to the waveguides.

2.5. Characterization of the sol–gel material and the resulting microstructures

In order to give some insight into the structure of the resulting doped polymer matrix, ^{29}Si NMR solid-state spectroscopy studies were carried out using a Bruker Avance 400 spectrometer. The sol–gel materials were obtained in bulk and grinded and sieved to get a particle size below 150 μm. Then they were spun at 10 kHz and spectrometer frequency was set to 79.49 MHz. Chemical shift values were referenced to tetramethylsilane (TMS). Spectra were recorded using a single-pulse sequence of

5 μs pulse time and 5 s waiting time between accumulations until approximately 400 accumulations were reached.

The quality of the patterns was evaluated by recording scanning electron microscopy (SEM) images using a Hitachi S-530 microscope that detects secondary electrons, following the deposition of a 10 nm-thick Au layer on top of the structures by vacuum evaporation.

2.6 Waveguide performance and sensor response

Absorbance measurements of substrate solutions (0.1 M acetate buffer containing 5×10^{-4} mol L^{-1} ABTS) containing 0.023 mg mL^{-1} HRP, in the absence and presence of H_2O_2 (1×10^{-4} mol L^{-1}) were carried out using a spectrophotometer (UV-2401PC, Shimadzu) in the visible region of the spectrum. PMMA cuvettes with a 1 cm path length were employed.

20 μm high waveguides were defined over silicon oxide substrates as described above. Evaluation of light confinement within these photonic structures was carried out. Light emitted from a pig-tailed LED ($\lambda = 670$ nm) was coupled to one end of the waveguides using a single-mode fibre optics. At the other end, at its focal position, a 15× optical microscope objective was placed, which allowed the obtaining of a magnification of the near field emerging from the waveguides. Such image was collected with a CCD camera (Pixelfly 200 XS VGA PCO AG, Germany). Once the image was obtained, 3D reconstruction of the intensity profile of the waveguide was done by using the software provided by SOLEX (SOLEX, Madrid, Spain).

For the evaluation of sensor performance, the CCD camera was replaced by a 50 μm diameter multimode fibre connected to a silicon photodiode (PD) (S1227-23BR Hamamatsu). Sensor response to H_2O_2 was recorded using a 0.1 M acetate buffer solution pH 5 containing 5×10^{-4} M ABTS and increasing concentrations of H_2O_2 in a range from 10^{-5} mol L^{-1} to 10^{-3} mol L^{-1}. A 4 μL drop of this solution was directly cast over the waveguide using a micropipette. Here, the solution penetrated into the waveguide core, due to the porous nature of the sol–gel material, thus reaching the embedded HRP. Once the substrate solution was cast, the output light power was recorded for 20 min for each concentration. The analytical measurement was taken after the first five minutes so as to allow the signal to stabilize. Previous to the performance of a new measurement, the biosensor was thoroughly rinsed with fresh 0.1 M acetate buffer pH 5 and deionised water, and dried under a N_2 stream. After each measurement the buffer solution was dispensed again and the signal was recovered within the experimental error.

3. Results and discussion

HRP-doped hybrid sol–gel glasses were prepared in an alcohol-free medium, in the absence of any catalyst, by hydrolysis and polycondensation reactions of methyltrimetoxysilane (MTMOS), phenyltrimethoxysilane (PhTMOS) and tetramethoxysilane (TMOS), at room conditions. The proportion of each component was optimized, with the aim of obtaining long, mechanically stable three-dimensional structures with good optical properties.[16] Indeed, MTMOS is known to be responsible for the mechanical integrity of the formed sol–gel structures by preventing the formation of fractures, cracks or defects on the material surface during the ageing and drying processes. However, MTMOS gives rise to sol–gel materials with a marked hydrophobic character. This effect can be tuned with the incorporation of TMOS, which confers the hydrophilic character required for sensing applications. Albeit, TMOS is also responsible for the shrinkage of the obtained structures, therefore the concentration of this monomer should not exceed a given value. The tuning of the optical properties is addressed with the introduction of PhTMOS. It has been previously reported how the variation of the proportion of this monomer enables the modification of the refractive index of the resulting material.[17]

During the process of preparation of the sol solution, methanol generated by the hydrolysis of the different silane monomers was eliminated from the solution together with water. In order to do that, the initial solution was stirred for up to 20 h until it lost around 40% of its initial weight. This was important in order to make the mixture suitable for the incorporation of a biomolecule. Once the HRP enzyme used in this work was added to the sol solution, this was kept in a sealed container and stored in the fridge at 4 °C. The sol solution was stable for several days. In addition, the HRP activity was tested during this period showing that negligible loss of activity occurred.

^{29}Si NMR solid-state spectroscopy studies provide information on the degree of condensation in the resulting polysiloxane matrix.[18,19] The number of siloxane bonds that surround each silicon atom is determined from characteristic signals. Si atoms from organotrialkoxysilanes, MTMOS and PhTMOS, can only form a maximum of three siloxane bonds and are responsible for T^n signals at chemical shift values in the region of −45 ppm to −70 ppm, where n indicates the number of bridging oxygens around the Si atom. On the other hand, Si atoms from TMOS can participate in a maximum of four bonds, being related to Q^n signals in the spectra. However, in this study Q^n signals are hardly observed due to the low content of TMOS in the starting alkoxysilane mixture. For instance, the ^{29}Si NMR spectrum of the unmodified xerogel (Fig. 1a) shows signals at −55.7 ppm and −64.4 ppm assigned to T^2 and T^3 signals, respectively, as well as a low intensity signal at −101.2 ppm attributed to Q^3. The relative areas of T^3/T^2 signals in this material are 52/48, indicating a significant degree of condensation, with 52% of Si atoms involved in three Si–O–Si bonds. The polycondensation of hydrolyzed alkoxysilanes is affected by the addition of the enzyme. The volume of HRP hinders the bridging of Si atoms, leading to a slight decrease in the relative intensity of the T^3 sites with respect to those of T^2, as previously observed for the encapsulation of glucose oxidase[20] and lipase[21] in different polysiloxane matrixes. The presence of HRP hampers the formation of siloxane bonds resulting in less cross-linked xerogels with T^3/T^2 relative values of 46/54 (Fig. 1b). However, this fact affects neither the macroscopic structure of the waveguides nor their light confinement ability, as will be shown below.

SEM images of the fabricated strip waveguides are presented in Fig. 2. They have very smooth surfaces with no cracks or defects, which confirm the quality of the obtained hybrid material. It can also be seen that there is an excellent replication from the used mould and that arrays of waveguides with different widths can be easily obtained with this fabrication technique.

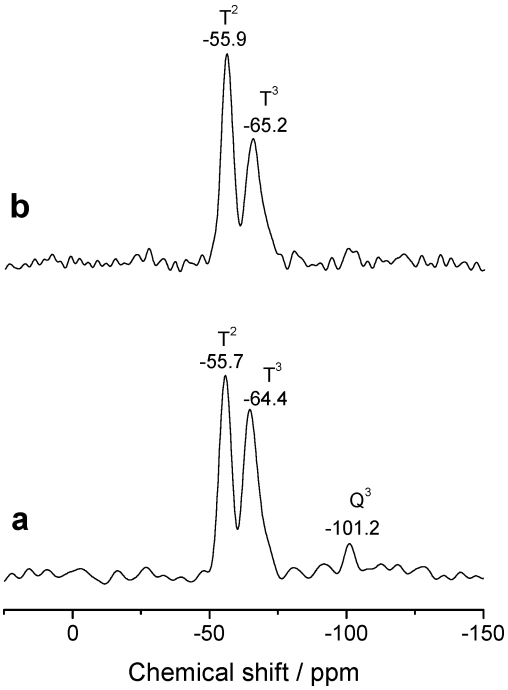

Fig. 1 ^{29}Si NMR spectra of the non-modified (a) and HRP-doped (b) xhybrid sol–gel materials.

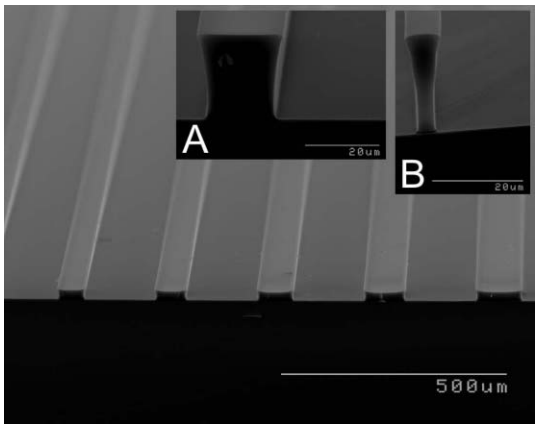

Fig. 2 SEM image of HRP-doped hybrid sol–gel waveguides patterned using MIMIC technique. Inset A and B show close-up images of the facet of cleaved waveguides of different height-to-width aspect ratios (20 : 15 and 20 : 3, respectively).

From these results, it is anticipated that such formulation is adequate for the fabrication of integrated optical systems; however, the existence of fractures, imperfections, aggregates, phase separation or nucleation points inside the waveguides, could lead to scattering/absorption centres. By cleaving the waveguides at a random position and taking a close-up picture of the facet ends (insets of Fig. 2), none of the undesired formations were observed and hence it can be concluded that the proposed material is suitable for defining integrated optical systems. Additionally, the insets of Fig. 2 also show a good mechanical stability of the material, which allows obtaining structures with high aspect ratios (>6 : 1).

Sensor performance is based on the use of colourless 2,2′-azino-bis(3-ethylbenzthiazoline-6-sulfonic acid) (ABTS) HRP co-substrate. The catalytic reduction of H_2O_2 takes place with the concomitant oxidation of ABTS to give the green-coloured cation radical $ABTS^{\bullet+}$ product. When a solution containing ABTS and H_2O_2 is dispensed over the HRP-doped sol–gel strip waveguide, the product is mainly obtained inside the photonic structure. Hence, if the appropriate wavelength is coupled to the waveguide, the measured absorbance depends on the amount of product generated during the catalytic reaction. Thus, the change in the absorption of the working wavelength in the waveguide as a function of the H_2O_2 concentration can be measured.

Absorbance spectra recorded in ABTS solutions, in the absence and presence of H_2O_2 are shown in Fig. 3. As it can be observed, in the absence of H_2O_2, the absorbance is very low in all the studied wavelength range. Conversely, when 10^{-4} mol L^{-1} of analyte is included in the solution, three peaks are present in the absorbance spectra (416 nm, 648 nm and 749 nm). From these values, an absorbance change of 1.2 a.u. at the chosen working wavelength ($\lambda = 670$ nm) confirms the validity of the proposed sensing approach.

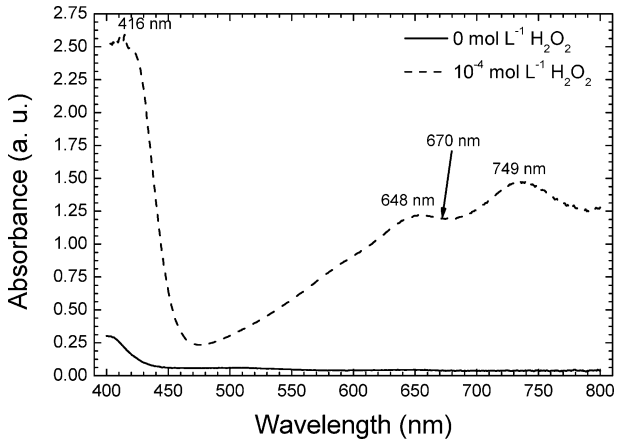

Fig. 3 Absorbance spectra of HRP-ABTS reaction medium containing 0 mol L^{-1} and 10^{-4} mol L^{-1} H_2O_2.

Fig. 4 shows the 3D reconstruction of the modal profile, that is, the power distribution of the light beam at the waveguide output. Such an image was obtained from the raw data (see inset) collected by the CCD camera after an acquisition time of 1 ms. Clearly, light remains well confined inside the sol–gel waveguide, since most of the light propagates inside the structure and only a small fraction, the evanescent field, is propagating outside it. The highly multimode behaviour, noticeable on the multilobular shape of the propagating light (the higher the lobe, the higher the intensity), was expected due to the waveguide dimensions and does not affect the overall working mechanism of the proposed chemical biosensor. Hence, the results presented in Fig. 4 confirms the suitability of both the material and the fabrication process.

As it was previously mentioned, doped sol–gel glasses for photonic biosensing applications have only been used in EF configuration.[11,12] Therefore, they do not require light confinement in the sensing layer. By contrast, the sensor configuration presented here requires the light confinement in the waveguide structure. A comparison between both approaches evidences a different light interaction with the target analyte. Whereas in the former, it is the EF that interacts with the analyte, in

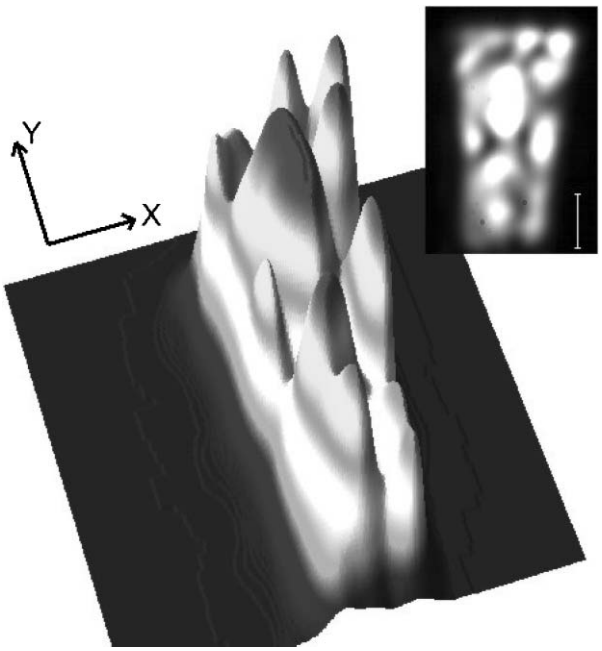

Fig. 4 Near-field reconstruction of the light propagating inside the waveguide obtained with the HRP-doped hybrid sol–gel material. Inset: image obtained with the CCD camera. The white line corresponds to 5 μm.

our sensor this interaction takes place with the entire wavefront coupled to the waveguide (and hence, they could be called full-field (FF) sensors, by analogy to EF sensors). This configuration requires minor propagation distances in order to achieve the same sensitivities as the EF configuration. Then, small and more densely packed sensors could be defined, which opens up the possibility of implementing high-throughput screening (HTS) sol–gel based (bio)chemical sensors. Additionally, working with strip waveguides, which confer 2D light confinement, packed sensor arrays could be defined for multianalyte detection using the same sol–gel material doped with different recognition elements.

Sensor performance was finally tested for a waveguide 20 μm high, 80 μm wide and 5000 μm long. Measurements were recorded as schematized in Fig. 5. Two fibre optics were used: the input fibre optics was responsible for coupling the working wavelength to the system while the output fibre optics brought the emerging light from the system to the PD. Once both fibres were aligned, solutions containing increasing concentrations of H_2O_2, in a range from 10^{-5} mol L^{-1} to 10^{-3} mol L^{-1} were

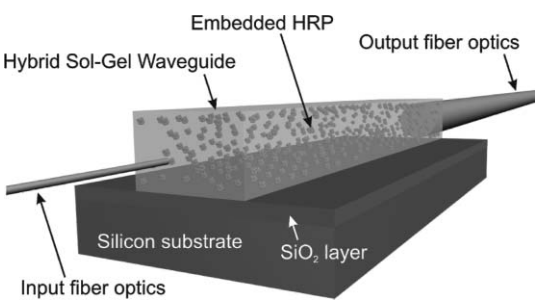

Fig. 5 Scheme of the sensor setup, with the input and output fibre optics aligned to the HRP-doped hybrid sol–gel waveguide.

directly dispensed over the sensor, simultaneously recording the power variation. After the whole set of measurements was done, the blank solution was cast again to confirm that there was no drift of the base signal. The corresponding calibration curve is presented in Fig. 6. As it can be observed, there is a good agreement with the linear behaviour predicted by the Beer–Lambert Law[22] in the range of 10^{-5} mol L^{-1}–3×10^{-4} mol L^{-1} H_2O_2, with an experimental sensitivity of $(3.1 \pm 0.2) \times 10^3$ a.u./mol L^{-1} and a SNR ranging from 17 dB to 15 dB depending upon the analyte concentration. It should be noted that the linear fit does not intersect the origin of coordinates. This can be understood if it is considered that the stock solutions of the substrate used (ABTS) always have a slight absorption at the working wavelength (slightly green-coloured due to the spontaneous oxidation of ABTS), which causes the sensor to not have zero absorbance when using the blank solution, as it was shown in Fig. 3. Then, instead of applying the 3σ IUPAC definition for determining the limit of detection (LOD)[23] of the sensor, a more realistic value was obtained using error propagation.[24] This method provides a LOD of 4.44×10^{-5} mol L^{-1} for this highly compact photonic biosensor obtained by the doping of a sol–gel glass with HRP. The sensor performance compares well with other published H_2O_2 sensors, based on both electrochemical[25] and optical[26] detection modes, which make use of HRP-doped polymer matrixes just as recognition elements in a more conventional configuration.

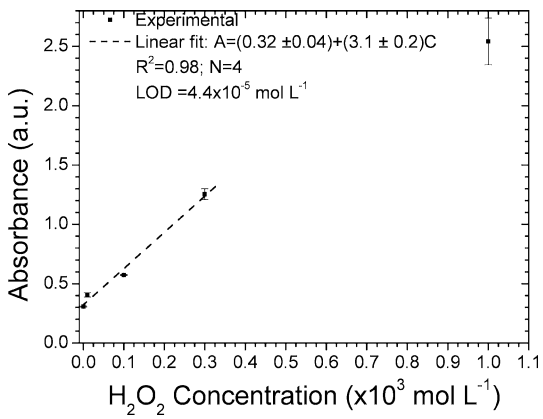

Fig. 6 Experimental results of the absorbance *vs.* H_2O_2 concentration for the waveguide biosensor, together with their respective linear fit and LOD.

4. Conclusions

A new approach for the fabrication of compact photonic lab-on-a-chip systems is described. The use of bio-doped hybrid sol–gel polymers enabled the full integration of both transducer and recognition elements into one single microstructure. High-quality strip waveguides of these materials were defined by MIMIC and proved to be an excellent configuration for the development of sensor approaches. We demonstrate the potential of this generic approach by developing a full-field photonic biosensor for the detection of H_2O_2 using HRP as the doping agent. This is a very promising versatile technology that combines tailor-made doped sol–gel materials and a one-step soft lithography fabrication approach which provides a general

way of developing cost-effective highly integrated photonic microsensor platforms.

Acknowledgements

This work was supported by CSIC (Spain; Proyectos Intramurales de Frontera 2005, project no. 200560F0142) and MEC-DGI (project no. CTQ2006-14644-C02/BQU). A. L and C. F-S. acknowledge the Spanish Ministry of Science and Education for the award of a Ramón y Cajal contract. M.D. acknowledges the CSIC for an I3P postdoctoral contract. V. J. C. acknowledges the CSIC for the award of a studentship of the I3P program. We also thank Dr I. Sobrados for technical assistance and fruitful discussions in the NMR study.

References

1 F. Prieto, B. Sepúlveda, A. Calle, A. Llobera, C. Domínguez, A. Abad, A. Montoya and L. M. Lechuga, *Nanotechnology*, 2003, **14**(8), 907.
2 A. Llobera, R. Wilke, D. W. Johnson and S. Büttgenbach, *IEEE Photon. Technol. Lett.*, 2005, **17**(12), 2628.
3 L. Yang, S. S. Saavedra, N. R. Armstrong and J. Hayes, *Anal. Chem.*, 1994, **66**, 1254.
4 C. Marzolin, S. P. Smith, M. Prentiss and G. M. Whitesides, *Adv. Mater.*, 1998, **10**(8), 571.
5 F. Pang, X. Han, F. Chu, J. Geng, H. Cai, R. Qu and Z. Fang, *Sens. Actuators, B*, 2007, **120**, 610.
6 E. Z. Faraggi, Y. Sorek, O. Levi, Y. Avny, D. Davidov, R. Neumann and R. Reisfeld, *Adv. Mater.*, 1996, **8**(10), 833.
7 J. H. Kim, B. W. Dudley and P. J. Moyer, *J. Lightwave Technol.*, 2006, **24**(1), 612.
8 Y. Chao, L. Shi, J. Wang and D. Lo, *Appl. Phys. Lett.*, 2003, **83**(20), 4101.
9 X. Orignac, D. Barbier, X. M. Du, R. M. Almeida, O. McCarthy and E. Yeatman, *Opt. Mater. (Amsterdam)*, 1999, **12**, 1.
10 H. Zang and M. Fallahi, *Opt. Commun.*, 2005, **248**, 415.
11 L. Yang and S. S. Saavedra, *Anal. Chem.*, 1995, **67**, 1307.
12 M. Zourob, S. Mohr, P. R. Fielden and N. J. Goddard, *Lab Chip*, 2005, **5**, 772.
13 R. Houbertz, L. Fröhlich, M. Popall, U. Streppel, P. Dannberg, A. Bräuer and B. N. Chichkov, *Adv. Eng. Mater.*, 2003, **5**(8), 551.
14 M. Casalboni, F. Belli, M. Cirillo, F. De matteis, P. Prosposito and R. Russo, *J. Sol–Gel Sci. Technol.*, 2003, **26**, 937.
15 Y. Xia and G. M. Whitesides, *Angew. Chem., Int. Ed.*, 1998, **37**, 550.
16 C. Fernández-Sánchez, V. J. Cadarso, M. Darder, C. Domínguez and A. Llobera, *Chem. Mater.*, 2008, **20**, 2662–2668.
17 S. Jeong, W. H. Jang and J. Moon, *Thin Solid Films*, 2004, **466**(1–2), 204.
18 R. H. Glaser, G. L. Wilkes and C. E. Bronnimann, *J. Non-Cryst. Solids*, 1989, **113**, 73.
19 P. Lacan, C. Guizard and L. Cot, *J. Sol–Gel Sci. Technol.*, 1995, **4**, 151.
20 A. Jimenez-Morales, PhD thesis, *Universidad Carlos III*, Leganés, Madrid, 1999.
21 C. M. F. Soares, O. A. A. dos Santos, H. F. de Castro, J. E. Itako, F. F. de Moraes and G. M. Zanin, *J. Non-Cryst. Solids*, 2006, **352**, 3469.
22 W. Göpel, J. Hesse, J. N. Zemel, E. Wagner, R. Dändliker and K. Spenner, in *Volume 6: Optical Sensors*, Wiley-VCH, Weinmeim, Germany, 1991.
23 V. Thomsen, D. Schatzkein and D. Mercuro, *Spectroscopy*, 2003, **18**(12), 112.
24 G. L. Long and J. D. Winefordner, *Anal. Chem.*, 1983, **55**(7), A712.
25 T. Tangkuaram, C. Ponchio, T. Kangkasomboon, P. Katikawong and W. Veerasai, *Biosens. Bioelectron.*, 2007, **22**(9–10), 2071.
26 K. M. Wang, J. Li, X. H. Yang, F. L. Shen and X. Wang, *Sens. Actuators, B*, 2000, **65**(1–3), 239.

